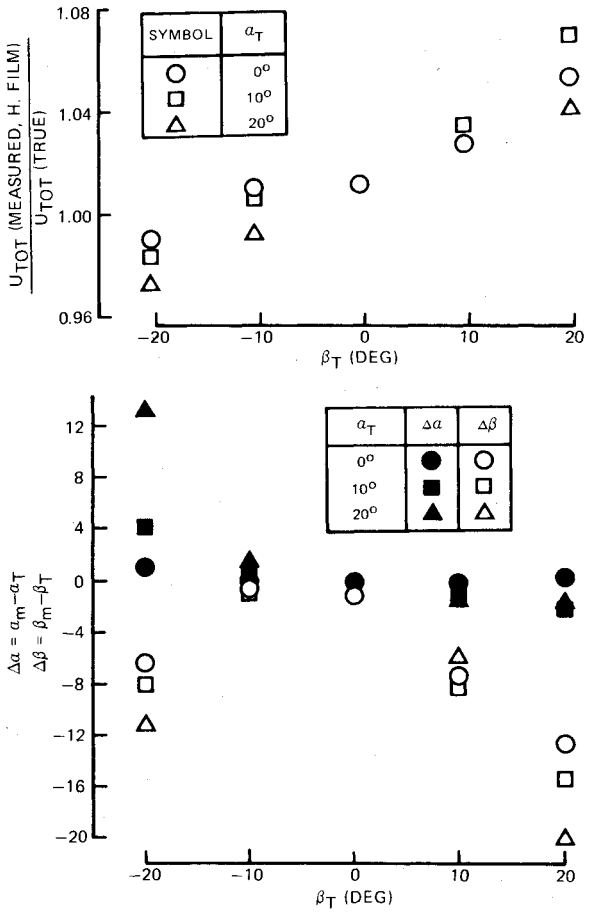

Fig. 2 Errors with K^2 formulation.

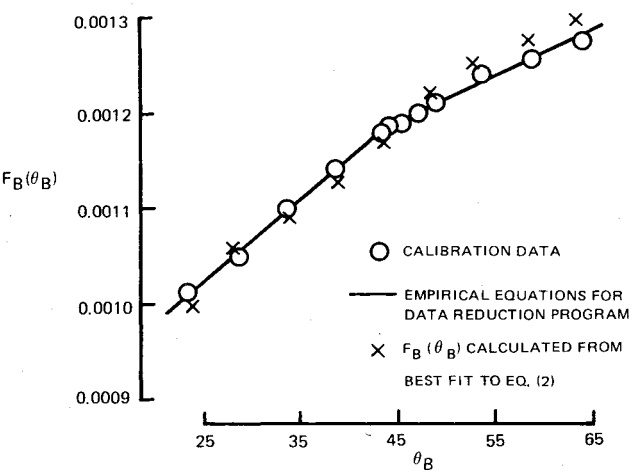

Fig. 3 Typical hot-film F calibration.

alternative to the angle-sensitivity formulation of Eq. (2), the velocity coefficient B of Eq. (1) is expressed by

$$B = B_0 F(\theta_i) \tag{4}$$

where the angle e_i is defined by

$$\cos\theta_i = (\hat{e}_i \cdot U_{tot})/U_{tot} \tag{5}$$

with $\hat{e}_i$ the unit vector in the direction parallel to the individual sensor, and U_{tot} the total velocity vector. One advantage of this type of formulation is simplified definition of angle relative to the previous use of two angles, α and β. The use of the angles $\theta_i - i = 1,2,3$ for the probe configuration of Fig. 1 was found to collapse the calibration data for α and β to a single curve for all sensors.

An example of such a calibration is given in Fig. 3 for the B sensor of Fig. 1. Note that, for these calibration data, the empirical equations used to describe the results represented the data to an accuracy of 0.5% or better. Although not shown, the calibrations $F_i(\theta_i)$ for all three sensors (Fig. 1) on all probes calibrated had calibrations similar to that of Fig. 3. A two-regime using straight lines permitted a simplified representation within the data reduction program. The specific calibration curve showing F vs θ_i would not be expected to be universally applicable and would depend on the particular sensor configuration employed. Since the value of $F_i(\theta_i)$ is used, and not the slope of the curve, the discontinuity in shape shown in Fig. 3 is of no relevance to the data reduction.

The change in slope probably is associated with the response of the hot-film sensors at large angles and directly related to the previously mentioned variability in value of constant K in Eq. (2). The step change in slope simplifies the data reduction procedure. Since no mechanism is readily apparent, one would expect a continuous change in slope between the two regions of constant slope. To emphasize the value of this new F formulation, the equivalent expression for $F_i(\theta_i)$ based upon the best fit of the data to Eq. (2) with constant K value is also shown on Fig. 3. To be sure, as an alternative to the F formulation, one could input a $K(\theta_i)$ expression into the data reduction as well; consideration of this alternative led to the conclusion that such a technique was unnecessarily complicated compared to the technique actually used.

Using the *same* data of Fig. 2 but with the new formulation, the results showed agreement to within less than 1% in total velocity and less than 1 deg in pitch or yaw angle (i.e., velocity direction). These accuracies, over a range of ±20 deg in flow direction, significantly increase the accuracy of subsequent calculations of performance in rotating machinery. As such, the technique represents an improvement in measurement techniques for unsteady flows for which accuracy is a more important requirement than frequency response.

References

[1] Bennett, J.C., "Use of Five-Hole Pneumatic Probe in Unsteady Flows," *Progress in Astronautics and Aeronautics: Experimental Diagnostics in Gas Phase Combustion Systems,* Vol. 53, edited by B.L. Zinn, AIAA, New York, 1977, p. 7.

[2] Bennett, J.C., "Measurements of Periodic Flow in Rotating Machinery," AIAA Paper 77-713, 1977.

[3] Jorgensen, F.E., "Directional Sensitivity of Wire and Fiber-Film Probes—An Experimental Study," DISA Info. Ser., No. 11, 1971, p. 31.

Supersonic Flow over a Deep Cavity for a Laser Application

Peter Shen*
Northrop Corporation, Hawthorne, Calif.

FLOW disturbances generated by a supersonic flow over a deep three-dimensional alcove were studied experimentally. The cavity geometry under study is shown schematically in Fig. 1. The alcove has a cross section 14-cm wide and 40-cm in the flow direction (L) with an adjustable

Received Feb. 17, 1978; revision received Aug. 8, 1978. This paper is declared a work of the U.S. Government and therefore is in the public domain.

Index categories: Shock Waves and Detonations; Supersonic and Hypersonic Flow.

*Sr. Staff Engineer, High Energy Laser Systems Laboratory, Laser Systems Division, Hughes Aircraft Co., Culver City, Calif.

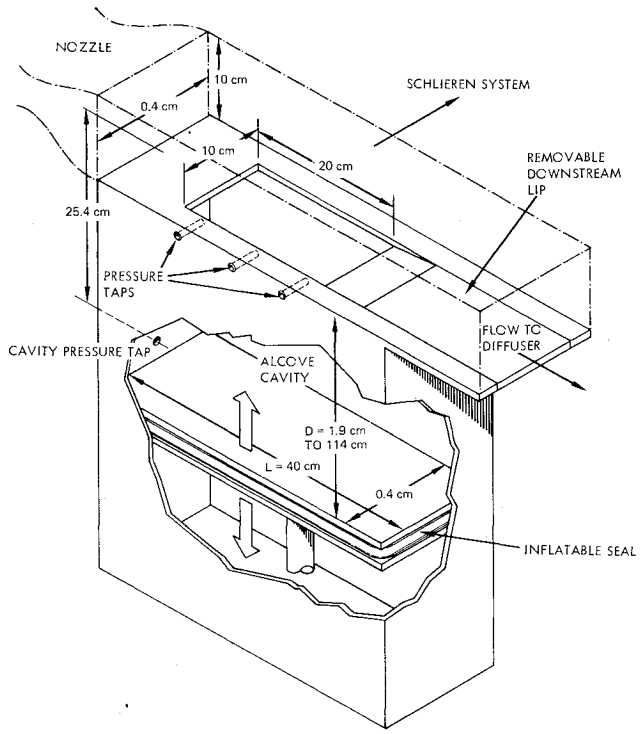

Fig. 1 Alcove schematic.

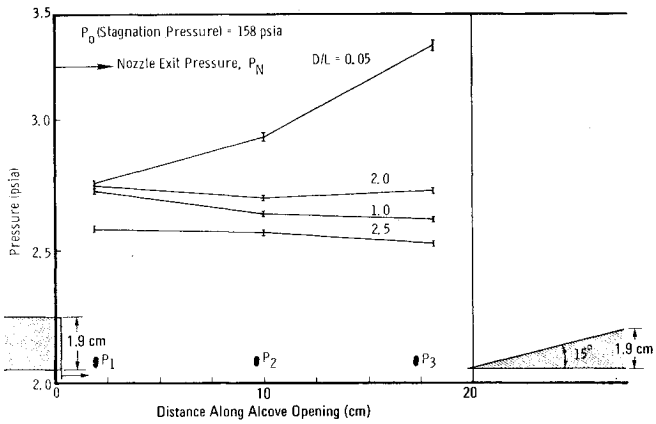

Fig. 2 Pressure distribution along alcove opening for various D/L ratios.

depth (D) to vary the D/L ratio. The alcove is centered around a 10 × 20 cm opening located 10-cm downstream of the Mach 3.2 nozzle exit. Dry nitrogen was chosen as the test gas. The turbulent boundary-layer thickness at the inlet of the alcove opening was calculated to be 0.84 cm. The calculated Reynold's number, based on the boundary-layer thickness and the recovery temperature, ranges from 2.9×10^5 to 3.2×10^5, depending upon the operating stagnation pressure.

Experiments were performed to obtain the optimum D/L ratio and downstream lip shape to give minimum pressure disturbances into the supersonic flow over the cavity. Flow disturbances were monitored by optical and pressure measurements along the opening of the alcove. The Validyne pressure transducer with 1-kHz frequency response was used to monitor the nozzle exit pressure. Three additional transducers were mounted along the alcove opening as shown in Fig. 1 to measure the pressure deviation from the nozzle exit pressure. One additional transducer is mounted on the side wall of the alcove cavity 25.4-cm below the opening to measure the alcove pressure.

A downstream lip of 15-deg wedge facing toward the supersonic flow was selected for the D/L ratio tests. Figure 2

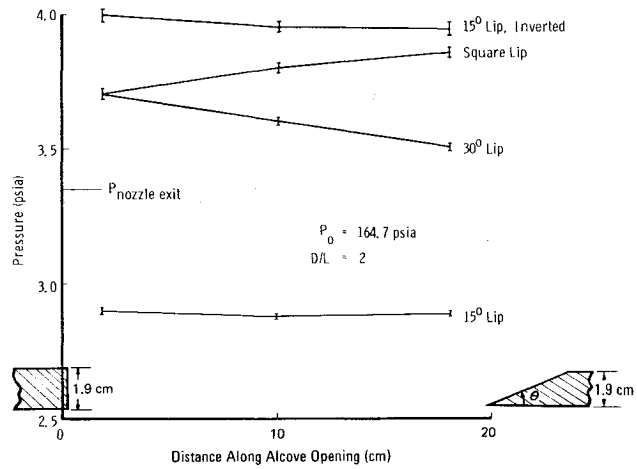

Fig. 3 Pressure distribution along alcove opening for various downstream lip shapes.

shows the pressure distribution along the alcove opening for various D/L ratios. It is indicated that for the 15-deg wedge, the average cavity pressure is always much lower than the nozzle exit pressure for all D/L ratios. These results are different from what Charwat[1] found for the two-dimensional rectangular cutout with the square downstream lip. The case of $D/L = 0.05$ represents typical shallow cavity characteristics where the recompression is indicated by higher P_3 than the nozzle exit pressure. The deep cavities with D/L ratios greater than 1 do not show the phenomenon of recompression. The maximum percentage change of pressure disturbance of Fig. 2, which is defined as $(P_{max} - P_{min})/P_{min}$, reduced to about 2% for D/L ratios greater than 2. It is noted that the pressure disturbances of small amplitude are proportional to the density disturbances, which are the direct measurement of the optical path difference of the laser beam propagating through a supersonic medium.

The second series of tests were conducted to evaluate the effects of various downstream lip shapes. Three additional lip shapes were selected for the tests. The square lip was selected to compare Charwat's[1] results on the rectangular cut out. The inverted 15-deg lip was selected to simulate the overhang lip which was found to give the lowest pressure disturbances in the shallow cavity.[2,3] A 30-deg wedge was selected to test the effect of the wedge angle on the flow characteristics in the cavity. Figure 3 shows that all three additional lips produce a higher alcove cavity pressure than the nozzle exit pressure. The Schlieren photographs indicate that a shock wave is generated from the leading edge of the cavity, instead of the expansion wave appearing in the case of the 15-deg lip. The three lips also produce higher pressure disturbances than the 15-deg lip.

By comparing the results of the 30-deg wedge and the 15-deg wedge, it was observed that the flow characteristics inside the alcove cavity change as the wedge angle increases from 15 to 30 deg. Figures 4 and 5 are Schlieren photographs showing the change of flow characteristics. Flow moves to the left. The first two diamond shocks can be traced back to the junction of the nozzle mated with the flow channel. The second oblique shock on the bottom plate results from the surface mismatch between a 4.5 in. × 9-in. glass plate insert and the bottom plate. These shocks are essentially Mach waves. The measured shock angles range from 18 to 18.5 deg. They should have minimum effects on the experimental results. The alcove opening is located on the top in the photograph. The dark fan in Fig. 4 indicates the expansion wave for the 15-deg downstream lip. The decrease in shear layer thickness indicates that the shear layer turns toward the cavity.

In Fig. 5, a different picture is shown. The dark fan is replaced by a white line, which indicates a shock instead of an expansion wave. Second, the shear layer is shown turned away

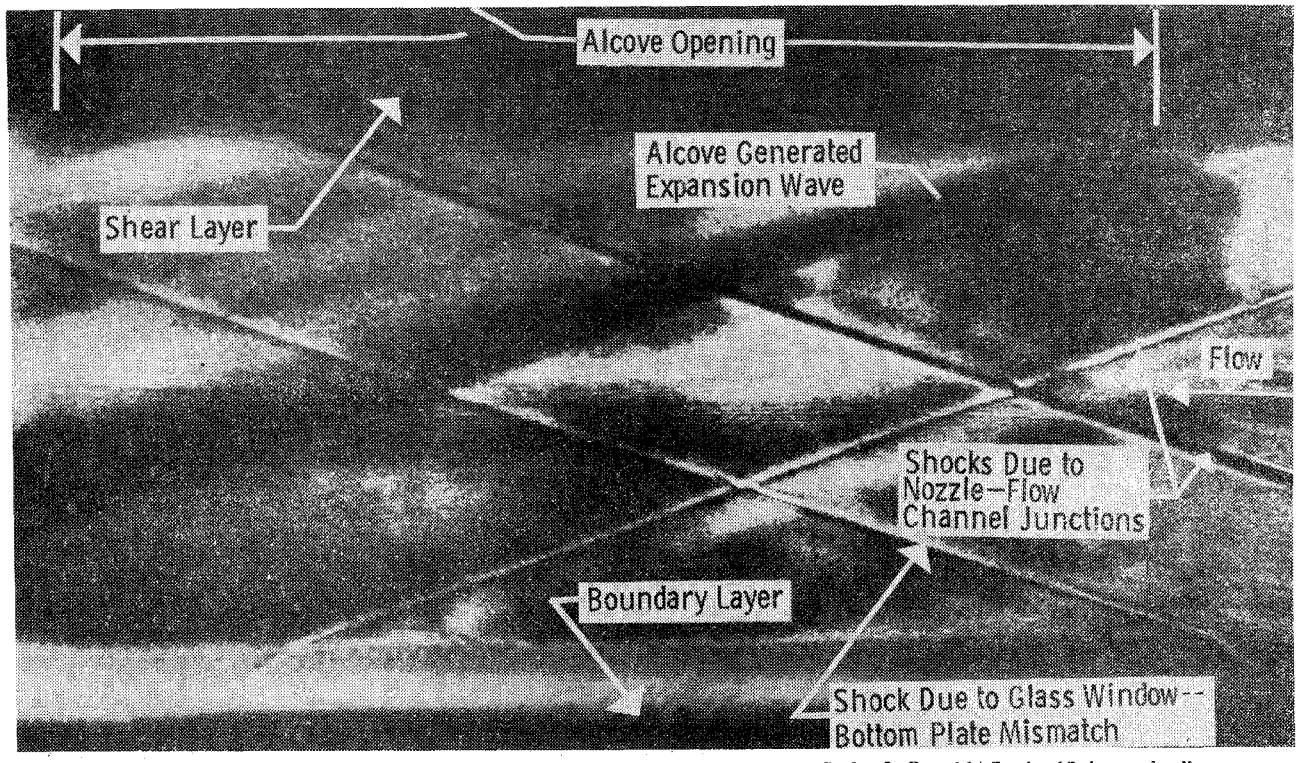

Fig. 4 Schlieren picture of pressure disturbances generated by alcove, $D/L = 2$, $P_0 = 164.7$ psia, 15-deg wedge lip.

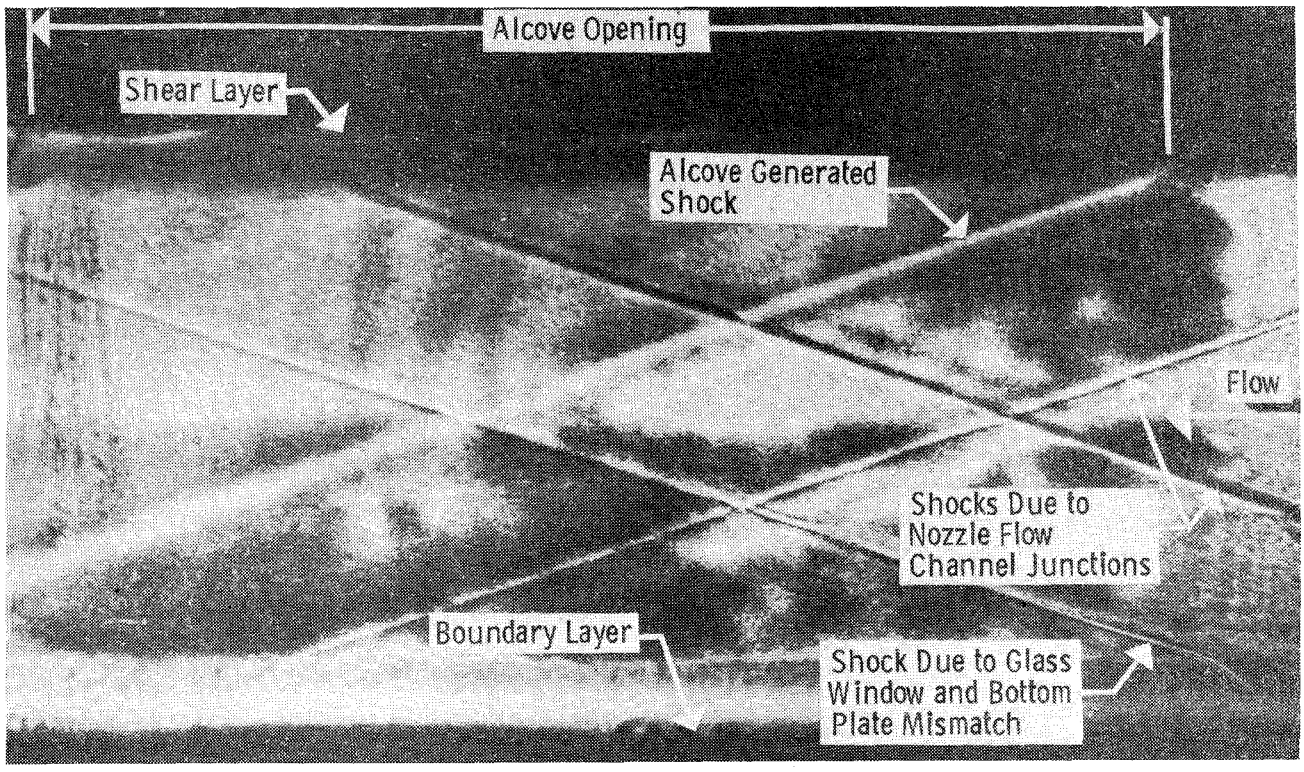

Fig. 5 Schlieren picture of pressure disturbances generated by alcove, $D/L = 2$, $P_0 = 164.7$ psia, 30-deg lip.

from the cavity. The change in flow characteristics may be contributed by flow reattachment on the downstream lip as the shear layer flow bridges over the cavity. As the shear layer flow reattaches to the downstream wedge surface, part of the flow is turned back into the cavity. The amount of flow turned back into the cavity depends upon the downstream wedge angle. For the 15-deg wedge, a small percentage of the mass in the shear layer is turned into the cavity. The leading-edge expansion dominates the cavity pressure. Consequently, the average pressure in the cavity is lower than the nozzle exit pressure, and the streamline bends toward the cavity. As the wedge angle increases from 15-deg, the shear layer flow turned back into the cavity increases, and it may over-compensate for the leading-edge expansion. The streamline, which is indicated by the shear layer, must turn away from the cavity to accommodate the excessive mass flow into the cavity. The higher pressure in the cavity is accommodated by a shock wave generated from the leading edge of the cavity.

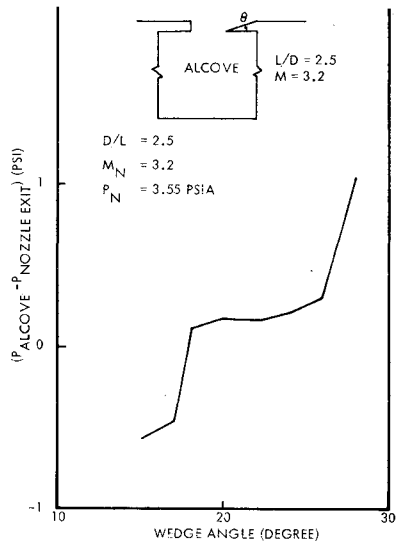

Fig. 6 Effects of downstream wedge angle on alcove cavity pressure.

This description is only qualitative and shock-boundary-layer interaction on the wedge surface may further complicate the flow characteristics inside the cavity.

Since the leading-edge wave, either shock or expansion wave, is not desirable as far as its effect on laser optical quality is concerned, efforts were directed to determining if it is possible to eliminate the leading-edge wave by an optimum choice of wedge angle between 15 and 30 deg, while preserving pressure uniformity. Further tests were performed using various wedge angles from 16 to 28 deg with increments of 2 deg (except for the 17-deg wedge). The results are shown in Fig. 6, where D/L ratio and stagnation pressure are selected to be 2.5 and 174.4 psia, respectively. It is shown that the average alcove cavity pressure is almost 1 psi higher than the nozzle exit pressure at the wedge angle of 28 deg. As the wedge angle decreases, the cavity pressure decreases with the wedge angle. At wedge angles between 18 and 24 deg the cavity pressure is relatively independent of the wedge angle and slightly higher than the nozzle exit pressure. However, the cavity pressure suddenly drops as the wedge angle decreases from 18 to 17 deg. At the wedge angle of 17 deg, the cavity pressure is almost 0.5-psi lower than the nozzle exit pressure. Further decrease in the wedge angle reduces the cavity pressure only slightly. The sudden increase in pressure between 17 and 18 deg may be caused by shock-boundary-layer interaction as the shear layer flow reattaches to the wedge surface. Analysis needed to give explanation of this phenomenon may be difficult in light of the three-dimensional nature of the alcove cavity. For all of the tests in Fig. 6, pressure uniformity along the cavity opening is in the range of 2 to 3%.

In conclusion, this study suggests that the geometric design of the deep cavity may have significant effects on the pressure disturbances generated by the cavity into the supersonic flow over the cavity, and that the design criteria for the deep cavity may be different from that of the shallow cavity. The minimum pressure disturbances may be obtained from the cavity design with D/L ratios greater than 2 and with its downstream lip shape of a wedge facing towards the supersonic flow. It is difficult to eliminate the pressure disturbances from the leading edge of the cavity. For the supersonic flow of Mach 3.2, the wedge angle between 18 and 24 deg should be selected, since the tolerance in the neighborhood of zero-strength wave from the leading edge is critical for practical purposes.

Acknowledgment

This work was supported in part by the Air Force Weapons Laboratory, Air Force Systems Command, U.S. Air Force, Kirtland Air Force Base, N. Mex. and the Defense Advanced Research Projects Agency (DARPA), Arlington, Va., on Contract F29601-75-C-0018.

References

[1] Charwat, A.F., Roos, J.N., Dewey Jr., F.C., and Hitz, J.A., "An Investigation of Separated Flows – Part I: The Pressure Field," *Journal of the Aerospace Sciences*, Vol. 28, June 1961, pp. 457-470.

[2] Petty, J., Private communication; Petty, J., Cooper, J., Kordegi, R., and Ortwerth, P.J., "The Use of Shaped Cavities to Improve the Side Wall Boundary Layer Quality in Gas Dynamic Lasers," *Laser Digest*, Fall 1974, AFWL-TR-74-344, pp. 202-230.

On the Accuracy of Linear Beam Theory

R. Parnes*
Tel-Aviv University, Ramat-Aviv, Israel

WHEN using the Bernoulli-Euler beam theory, $EI/R=M$, to calculate beam deflections, $y(x)$, the curvature term

$$\kappa \equiv \frac{1}{R} = \frac{y''}{[1+(y')^2]^{3/2}} \tag{1}$$

is usually linearized by assuming $|y'| \ll 1$, resulting in the linear relation for the elastic curve

$$EIy''(x) = M(x) \tag{2}$$

Although qualitative reasons for this assumption are usually given, no mention is made of the order of magnitude of the inaccuracy introduced. While it is true that comparisons can be made with Elastica solutions, expressed in terms of elliptic integrals, the complexity of these solutions precludes analytic expressions for the error and leads only to numerical comparisons.[1] On the other hand, the measure of the order of inaccuracy of the linear theory presented for the simple model given below leads to a simple relation for the error.

We consider a prismatic beam of flexural rigidity EI and length L, subjected to end couples M (Fig. 1). In this case, the elastic curve assumes a constant curvature and, from geometry, the exact displacement Δ of the midpoint C is:

$$\Delta = R(1-\cos\theta/2) \tag{3}$$

where θ is the subtended angle. Using the Bernoulli-Euler relation and the inextensible property of the elastic curve expressed by $R\theta = L$, we obtain

$$\Delta = \frac{EI}{M}\left[1-\cos\left(\frac{ML}{2EI}\right)\right] \tag{4}$$

Expansion of the cosine term as a Taylor series and retention of the first three terms yields

$$\Delta = \frac{ML^2}{8EI}\left[1-\frac{1}{48}\left(\frac{ML}{EI}\right)^2\right] \tag{5}$$

Received Feb. 9, 1978; revision received Aug. 14, 1978.

Index category: Structural Statics.

*Associate Professor, Dept. of Solid Mechanics, Materials and Structures, School of Engineering.